ZIBELINE INTERNATIONAL™ PUBLISHING

Water Conservation and Management (WCM)

DOI: http://doi.org/10.26480/wcm.02.2026.309.318

ISSN: 2523-5664 (Print)
ISSN: 2523-5672 (Online)
CODEN: WCMABD

RESEARCH ARTICLE

ENHANCING FLOOD MANAGEMENT AND WATER INFRASTRUCTURE EFFICIENCY: EXPERIMENTAL ANALYSIS OF DISCHARGE COEFFICIENTS IN CHUTE SPILLWAYS

Nabaa Noori Bashboosh*

Faculty of Engineering, Kufa University, Najaf, Iraq
****Corresponding Author Email: nabaan.shamsaldeen@uokufa.edu.iq***

Article History:

Received 11 March 2026
Revised 18 April 2026
Accepted 15 May 2026
Available online 12 June 2026

ABSTRACT

The impact of downstream face inclination on the discharge coefficient of chute spillways is thoroughly examined in this work using experimental investigation. Physical models were used in a series of controlled discharge laboratory tests where downstream face angles (θ = 30 °, 45 °, 60 °, and 70 °) were systematically varied in parallel. Twenty foam models with five different lengths of the crest (L_{cr}) values 10, 11, 12, 13, and 14 cm were created in the lab. Additionally, each model was attached to a plain stilling basin that measured 1 m in length (L_b) and 3 cm in depth. Every test was carried out in a lab flume that was 15 m long, 0.3 m wide, and 0.45 m high. The discharge values are 21.3, 20.9, 19.7, 19.3, 18, 15.6, and 14.8 l/s. A non-dimensional technique, according to Buckingham's theorem, linking the value of C_d as a dependent variable and other independent non-dimensional variables of $(\frac{H_{cr}}{P})$, $(\frac{L_{cr}}{y_c})$, θ, F_{r1}, and $(\frac{L_j}{L_b})$ was determined by dimensional analysis. SPSS v26 was used to process experimental data to determine a non-dimensional relationship between the coefficient of discharge and the other geometric and hydraulic non-dimensional parameters. The results also demonstrate how submergence conditions and downstream geometry interact on the value of C_d. A predictive association for C_d with a coefficient of determination of 0.955 is suggested based on the combined dataset, providing increased accuracy.

KEYWORDS

Coefficient of discharge, Chute spillway, Downstream face inclination, Froude number.

1. INTRODUCTION

Accurate prediction of the capacity of discharge over chute spillways plays a crucial role in the strategies of flood management. Any underestimation of the coefficients of discharge may lead to overtopping hazard, while overestimation may lead to making the design uneconomical. Therefore, improving the understanding of discharge coefficients contributes directly to enhancing the efficiency and safety of water infrastructure systems.

By including downstream face effects into discharge coefficient estimation, this study contributes to more effective and dependable spillway design and offers fresh insights into the hydraulic behavior of chute spillways (low ogee spillways). Considering the crest as a broad crested weir, very few studies have examined the value of the discharge coefficient at the crest of a chute spillway and connected it to geometric variables like the length of the crest, L_{cr}, and the angle of slope of the downstream face. The relationship between the discharge coefficient value and the depths created in the stilling basin due to the hydraulic leap phenomena was also examined in this study.

The impact of the approaching channel on the ogee spillway discharge coefficients with axial arches and converging walls was investigated by researchers. According to the findings, the discharge coefficient will rise by 22%, and the flow depth on the spillway crest will drop by 11% when the approaching channel's width is increased by 52% (Sheikh Kazemi and Saneie, 2014). The constructed laboratory models with geometric and hydraulic parameters similar to those of an arc-shaped ogee spillway and an ogee spillway oriented perpendicular to the flow. According to the first model's results, C_d rose to 1.72 when the water head to design head ratio grew. After spillway submergence, C_d dropped to 1.23. Furthermore, submergence occurs more quickly, and C_d will be lower for the same discharge levels in the spillway physical model with a normal form (Eshrati et al., 2015).

In order to simulate flow in spillways, researcher used a 3D numerical model. According to their findings, for ratios greater than 1.0, the discharge coefficients deviate by less than 1% from those suggested by USBR. The software determines a higher discharge capacity for lower values, which rises as the P/H ratio falls (Aguilera and Jimenez, 2019).

Other researcher examined the flow over an ogee spillway and connected their findings to the discharge coefficient, the length of the weir, and the upstream total head above the weir crest. In a recent study, number of parameters, including the weir's slope at upstream, the elevation of the apron, and the degree of submergence, affect the value of the coefficient of discharge. An ogee crest with a vertical face at upstream, ogee weirs have different values of inclination faces (18 °, 33 °, and 45 °). The thickness at the downstream apron is 3, 5, 7, and 10 cm in free flow, and an ogee weir with a vertical upstream slope under submerged flow. The results indicate that the discharge coefficient increases with increasing P/H_e and then

Quick Response Code	Access this article online	
	Website: www.watconman.org	**DOI:** 10.26480/wcm.02.2026.309.318

Cite The Article: Nabaa Noori Bashboosh (2026). Enhancing Flood Management and Water Infrastructure Efficiency: Experimental Analysis of Discharge Coefficients in Chute Spillways. *Water Conservation and Management, (WCM),* 10(2): 309-318.

remains a constant value. In submerged flow conditions, the value of the coefficient of discharge decreased from 2.25 to 2.15 (Salmasi and Abraham, 2022).

The study constructed a physical model to simulate the spillway of Condoroma dam at 4075 m a.s.l. The experimental work includes several conventional profiles of spillways with vertical faces of upstream with five values of dimensionless heights (P/H_d). The results show that the coefficient of discharge adjusted to the Condoroma altitude is lower than obtained from traditional formulae of conventional spillway design within a wide range of P/H_d ratios (Rendón et al., 2023).

This simulated a three-dimensional CFD model of the flow over a prototype spillway. The results with experimental data. The k-ε viscous standard model and the Volume of Fluid (VOF) approach were used in the numerical model. When the velocity values from the numerical model and the experimental data were compared, there was good agreement. Furthermore, cavitation index values were calculated based on pressure values that were derived from the numerical model. Because the index values were consistently above 0.2 throughout the cross-sections, the results showed that there was no cavitation risk in the prototype spillway (Varcin et al., 2025). The function of downstream face inclination in regulating the discharge coefficient has been largely overlooked in the majority of prior research, particularly when using experimental. Its connection with flow regime transitions and submergence circumstances has also received little consideration. This study is innovative because it systematically measures the impact of downstream face inclination on the discharge coefficient of chute spillways by using experimental data. In contrast to earlier research, this study provides a more thorough and design-focused understanding by establishing a direct relationship between downstream geometry and Cd while also taking submergence effects into account.

In practical hydraulic structures engineering, spillways represent a critical safety part in flood control systems. Their ability to convey excess water efficiently directly influences reservoir operation, dam safety, and mitigation of downstream risk. Therefore, improving the prediction of discharge is not only a necessity but also a key factor in the management of sustainable water infrastructure. The present study focuses on the gap between experimental hydraulic analysis and flood management applications by providing insights into how geometric modifications of chute spillways can enhance the efficiency of discharge under varying flow conditions.

The physical model to examine the hydraulic properties of Turkey's Kavsak Dam and Hydroelectric Power Plant (HEPP) for energy production was used. Experiments were carried out using the 1/50-scaled physical model. For various flow conditions, data on flow depth, discharge, and pressure were recorded. With the experimental investigation, significant changes were made to the initial project. Results from physical modeling and Computational Fluid Dynamics (CFD) simulation were used in comparative research to assess computational fluid dynamics' capacity to model spillway flow. The numerical model configuration was modeled using a commercially available CFD tool that solves the Reynolds-averaged Navier-Stokes (RANS) equations by defining cells in the computational space where the flow is either fully or partially confined. The outcomes of the numerical model and the physical model were compared using discharge rating curves, velocity patterns, and pressures. It was demonstrated that the flow properties of the numerical and physical models agree rather well (Kumcu, 2017).

2. Materials and Methods

As shown in Figure 1 below, a 3D sketch of the laboratory models used in the laboratory tests, while Figure 2 illustrates the basic governing geometric and hydraulic parameters:

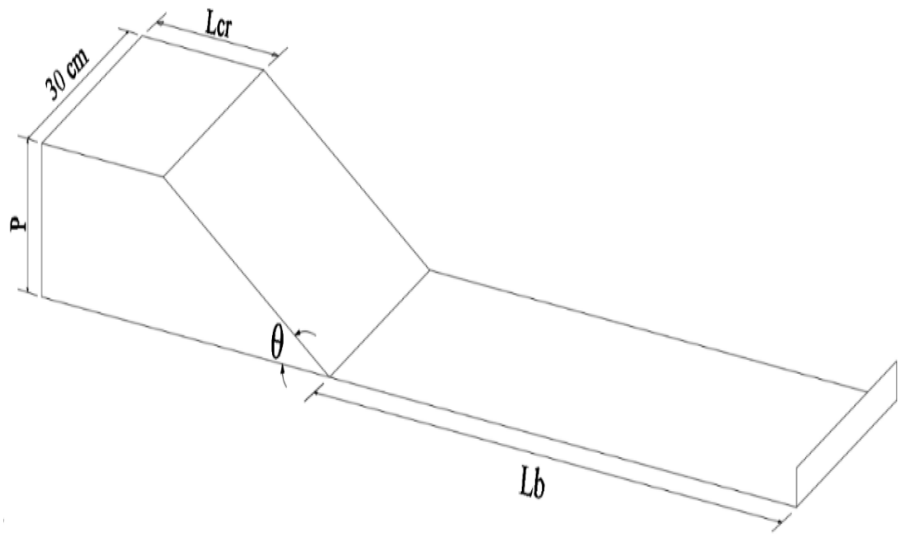

Figure 1: 3D sketch of the laboratory model

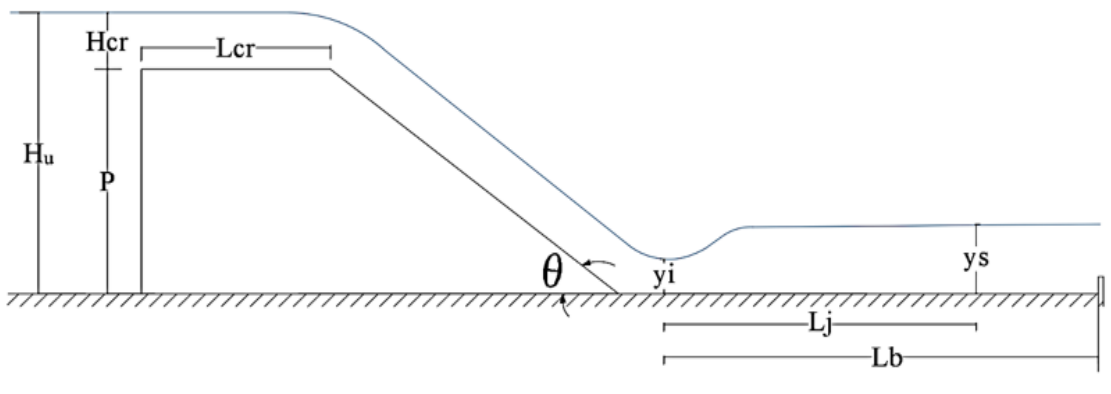

Figure 2: Side view sketch of the laboratory model

All laboratory models fabricated from foam with different dimensions are illustrated in Table 1 below:

Table 1: Details of laboratory models					
Model no.	θ °	L_{cr} (cm)	Model no.	θ °	L_{cr} (cm)
1	30	10	11	60	10
2	30	11	12	60	11
3	30	12	13	60	12
4	30	13	14	60	13
5	30	14	15	60	14
6	45	10	16	70	10
7	45	11	17	70	11
8	45	12	18	70	12
9	45	13	19	70	13
10	45	14	20	70	14

The flume was calibrated using a standard weir according to USBR specifications, for a standard sharp-crested 90° V-notch weir (USBR, 2001). For every model, the stilling basin's (L_b) length downstream of the spillway is one meter. A laboratory flume measuring 0.3 m in width, 0.45 m in height, and 15 m in length was used for all of the experiments. Figure 4 depicts the model during operation, whereas Figure 3 illustrates the flume's specifics.

Figure 3: The laboratory flume

Every lab model is fastened to the flume three meters away from the flume's main gate. Seven discharge values (0.0213, 0.0209, 0.0197, 0.0193, 0.018, 0.0156, and 0.0148 m^3/s) were applied to each model. To generate near-hydrostatic pressure distributions, a broad-crested weir has a flat crest that is much longer than the specific energy. The streamlines above the crest must be parallel to the crest, or straight (Henderson,1966; Chanson, 2004). With H_{cr} being the upstream head above crest and L_{cr} being the weir crest length shown in Figure 1, the dimensionless head above crest H_{cr}/L_{cr} should normally be between 0.1 and 0.50 (Govinda Rao and Muralidhar et al., 1963).

$$Q = \frac{2}{3}^{1.5} * C_d * b * \sqrt{2g} * H_{cr}^{1.5} \quad (1)$$

Q: actual discharge passing over the crest (m^3/s)

C_d: the coefficient of discharge

b: the effective width of the crest (m)

g: the gravitational acceleration (m/s^2)

H_{cr}: the head of water over the crest (m)

A critical flow transition zone where supercritical flow quickly transforms into subcritical flow, causing significant energy loss, is represented by the hydraulic jump that forms downstream of the spillway toe. This phenomenon has been thoroughly investigated in relation to energy dissipation efficiency and stilling basin design (Rajaratnam, 1990; Chow, 1959).The head over the crest (H_{cr}) is measured by subtracting the value of spillway height (P) from the head of water at the upstream side (H_u).

Figure 4: The laboratory model during run

3. Dimensional Analysis

The governing parameters that affect the discharge coefficient for the flow over the crest of the chute spillway can be written as:

$$C_d = f\ (H_{cr}, V_i, L_{cr}, L_j, P, \theta, \rho, g, \mu, \sigma, y_i, y_{cr}) \quad (2)$$

where ρ is the water density, μ is the water's dynamic viscosity, g is the acceleration due to gravity, σ is the surface tension, V_i is the flow velocity at the initial depth of the hydraulic jump created at the stilling basin, L_{cr} is the length of the crest, L_j is the length of the hydraulic jump, y_i is the initial depth of the hydraulic jump, y_{cr} is the critical depth, and θ is the spillway's downstream slope. All physical quantities that are defined with respect to an arbitrary constant value. Length (L), mass (M), and time (T) are three fixed dimensions that are of importance in mechanics of fluid. These fixed dimensions are called fundamental dimensions (Arora, 2005). The definitions of the other variables were given earlier. To derive additional useful dimensionless parameters, the Buckingham theorem was used. Because they encompass every dimension in the variables utilized in the dimensionless analysis, three iterative variables are chosen: ρ, Q, and yi. The following criteria describe the C_d as a function of these parameters after removing some non-effecting parameters and rearranging the others:

$$C_d = f\ (\frac{H_{cr}}{P}, \frac{L_{cr}}{y_{cr}}, \theta, F_{ri}, \frac{L_j}{L_b}) \quad (3)$$

C_d: the coefficient of discharge

$\frac{H_{cr}}{P}$: the non – dimensional of the head of water over the crest

$\frac{L_{cr}}{y_{cr}}$: the non – dimensional of the length of the weir

θ: The slope of the downstream face of the spillway

$\boldsymbol{Fr_i}$: the Froude number due to the initial depth of the hydraulic jump generated at the stilling basin

$\frac{L_i}{L_b}$: the non–dimensional length of the hydraulic jump

4. Results and Discussion

Raising the downstream face inclination eliminates flow interference close to the crest and lessens the backwater effect, allowing the flow to accelerate more freely. Also, when increasing the downstream face inclination, the coefficient of discharge (C_d) also increases. However, an excessive slope may cause flow separation, and the value of C_d may not change.

4.1 Relation of C_d vs. $\frac{H_{cr}}{P}$

From an engineering perspective, the reduction in C_d with increasing H_{cr}/P indicates a potential limitation in the capacity of discharge of the spillway during extreme values of flow conditions. This behavior is particularly critical in scenarios of flood, where higher upstream heads are expected. Therefore, designs operating within lower H_{cr}/P ratios are desired to maintain the discharge to be efficient and reduce the hazard of upstream water level rise.

Figures 5, 6, 7, and 8 show the results of experimental work for the first five models and for different values of θ = 30°, 45°, 60°, and 70°, which indicate an inverse nonlinear relationship between the relative critical depth (H_{cr}/P) and C_d. As can be seen, C_d decreases as H_{cr}/P values increase, proving that the hydraulic performance decreases as H_{cr}/P rises. The flow over the crest resembles optimal free-flow conditions when the values of H_{cr}/P decrease. The nappe is well-aerated, and the values of headloss become negligible as a result of turbulence and the separation of flow. Increasing the values of C_d is attained, and that indicate the effective characteristics of discharge. The flow depth increases over the crest, and a gradual deviation from optimal free-flow conditions results when increasing the value of H_{cr}/P.

Furthermore, even though the complete submergence is not satisfied, the flow approaches a partial state of submergence. In model number 16, the maximum value of C_d was 2.07, while the lowest value of H_{cr}/P was 0.1484. In contrast, model no. 5 had a maximum value of H_{cr}/P of 0.4161 and a minimum value of C_d of 0.6356.

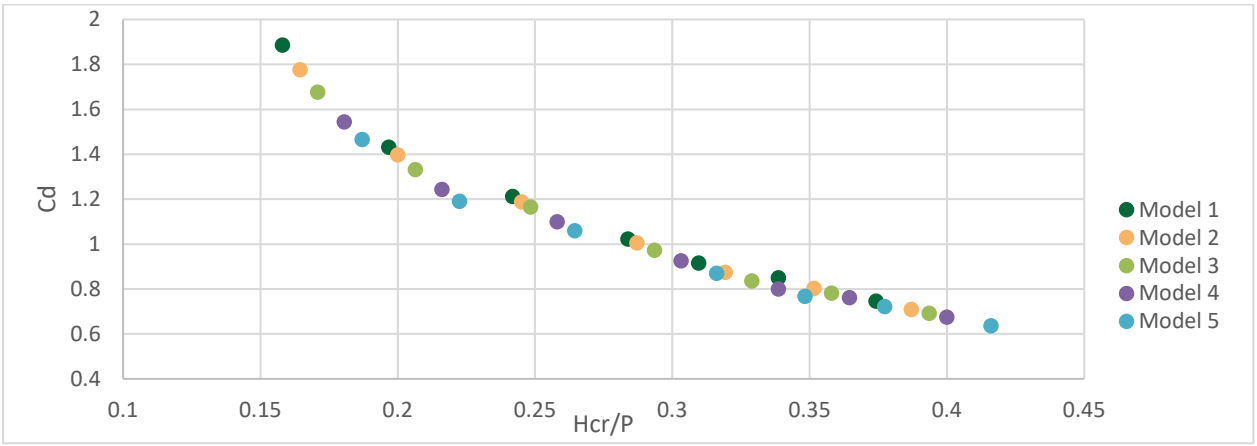

Figure 5: The relationship between C_d vs. $\frac{H_{cr}}{P}$ for θ = 30

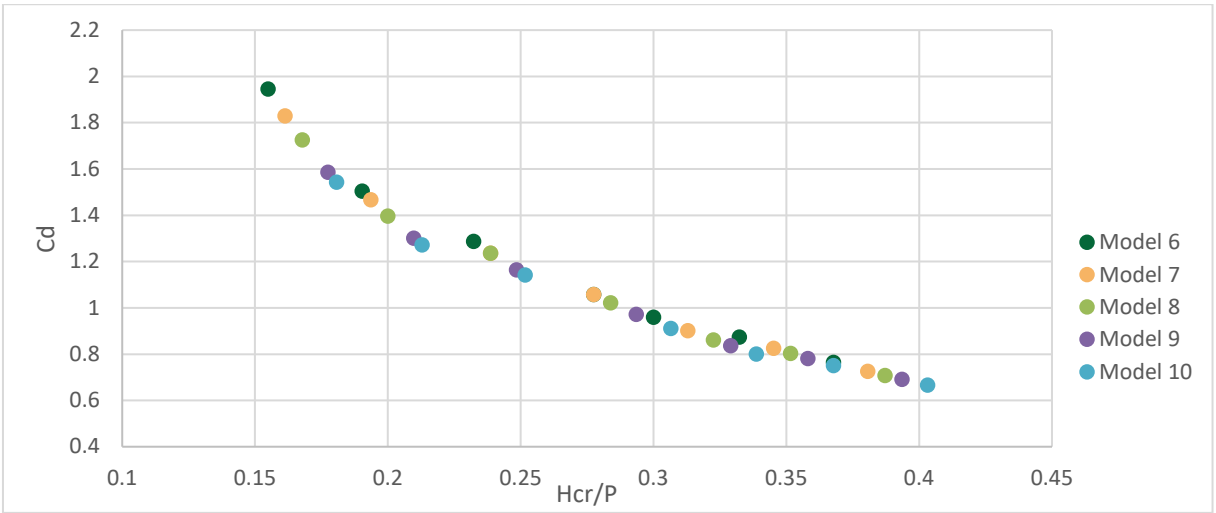

Figure 6: The relationship between C_d vs. $\frac{H_{cr}}{P}$ for θ = 45 °

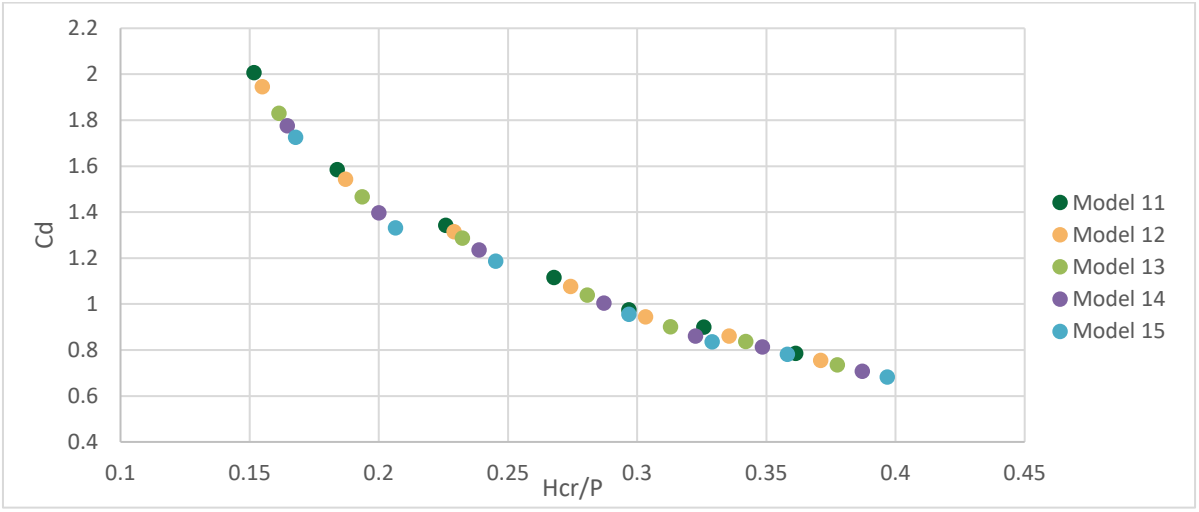

Figure 7: The relationship between Cd vs. $\frac{H_{cr}}{P}$ for θ = 60 o

4.2 Relation of C_d vs. $\frac{L_{cr}}{y_{cr}}$

This observation suggests that increasing of the length of the crest can enhance flow regulation and improve the stability of discharge. In practical applications, this can contribute to more controlled flood release, reducing the fluctuations of flow and improving the safety conditions at the downstream. Figures 9, 10, 11, and 12 show a dispersed distribution with no discernible monotonic trend.

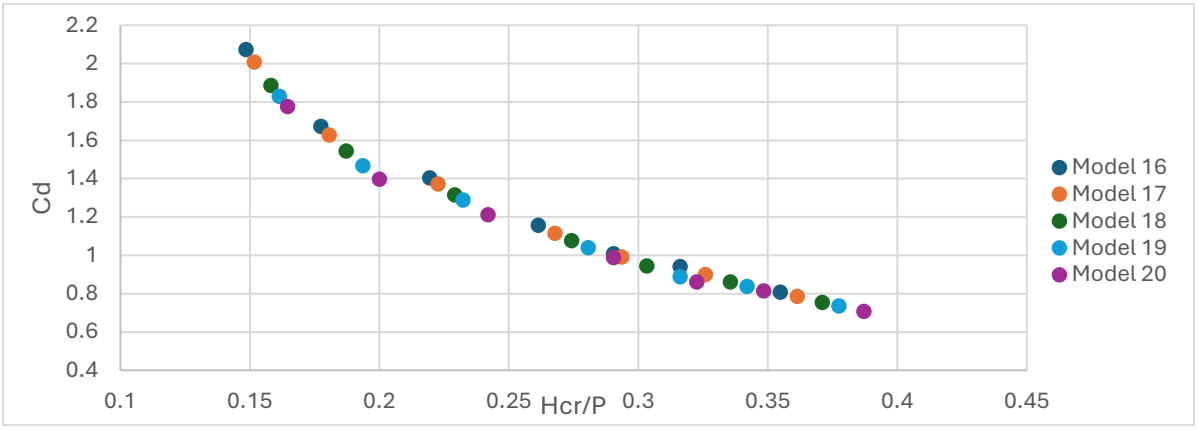

Figure 8: The relationship between C_d vs. $\frac{H_{cr}}{P}$ for θ = 70 °

In the relationship between the discharge coefficient (C_d) and the relative crest length (L_{cr}/y_{cr}) for the values of θ = 30°, 45°, 60°, and 70° . Nonetheless, a general trend of rising C_d with rising Lcr/ycr can be seen, especially at higher ratio values. The relative length of the weir crest in relation to the critical flow depth over the crest is physically represented by the parameter (L_{cr}/y_{cr}). The degree to which the flow changes and evolves as it crosses the crest is determined by this ratio. The establishment of a stable flow profile is restricted for small values of Lcr/yc because the crest length is comparatively short in relation to the flow depth. In these situations, the flow accelerates quickly, and the boundary layer is not fully developed, which increases flow instability and energy losses and results in lower C_d values. The results show that the maximum value of C_d at each model is recorded at the maximum value of L_{cr}/y_{cr}. The crest length long enough as L_{cr}/y_{cr} increases to make the flow at the zone of critical conditions. Increasing values of C_d lead to hydraulic performance becoming better, which is a result of the prolonged interaction between the flow and the surface of the crest. Figure 9: The relationship between C_d vs. $\frac{L_{cr}}{y_{cr}}$ for θ = 30 °

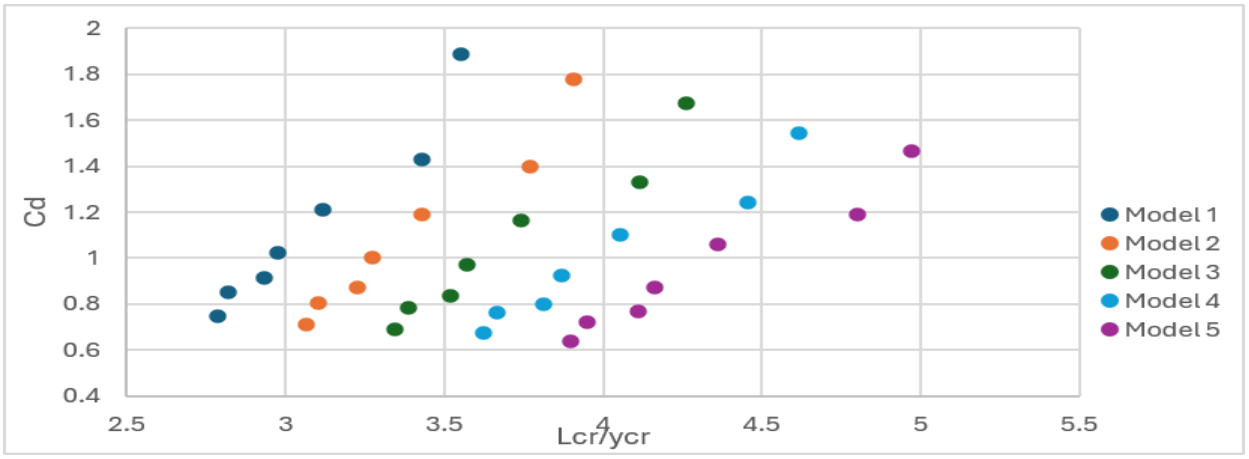

Figure 9: The relationship between C_d vs. $\frac{L_{cr}}{y_{cr}}$ for θ = 30 °

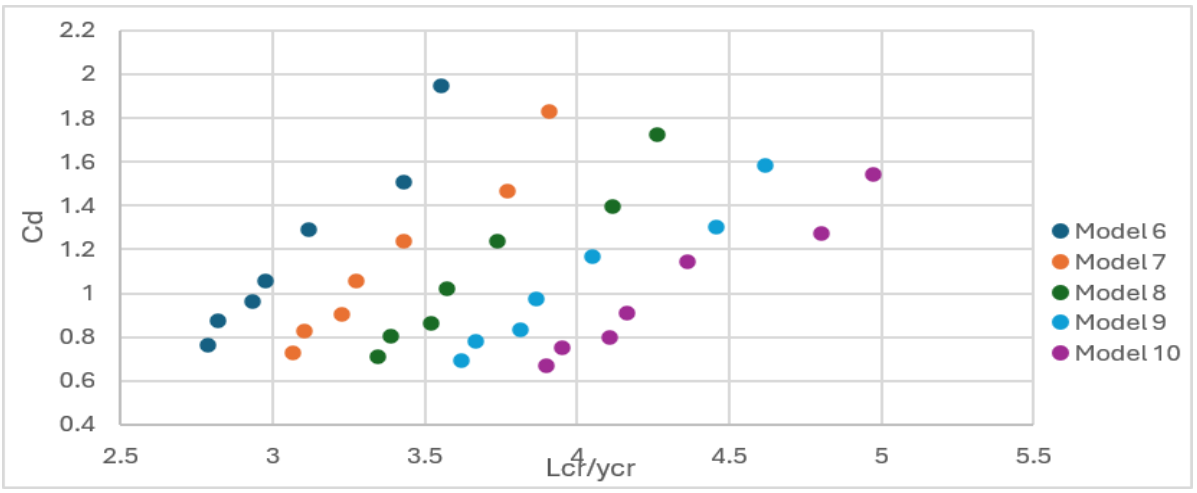

Figure 10: The relationship between C_d vs. $\frac{L_{cr}}{y_{cr}}$ for θ = 45 °

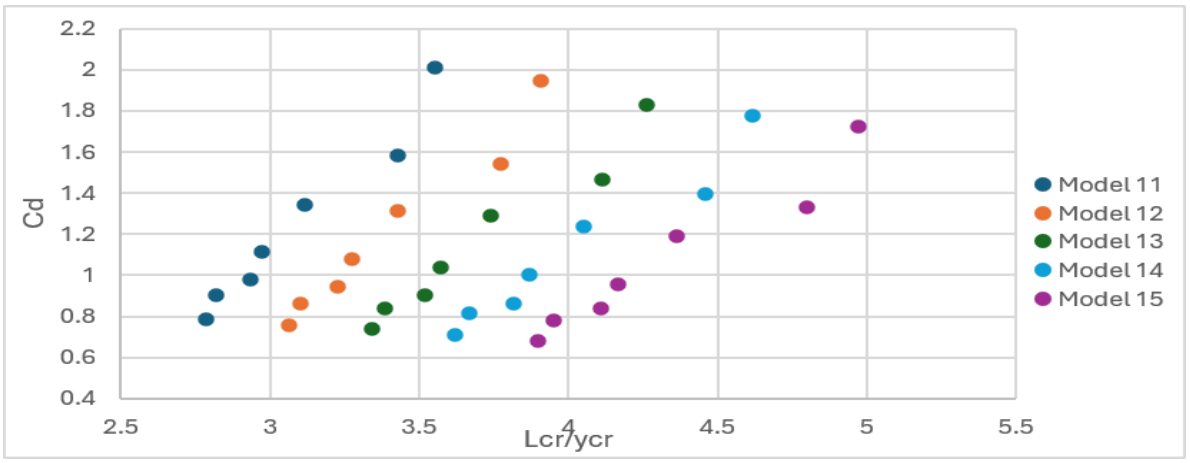

Figure 11: The relationship between C_d vs. $\frac{L_{cr}}{y_{cr}}$ for θ = 60 °

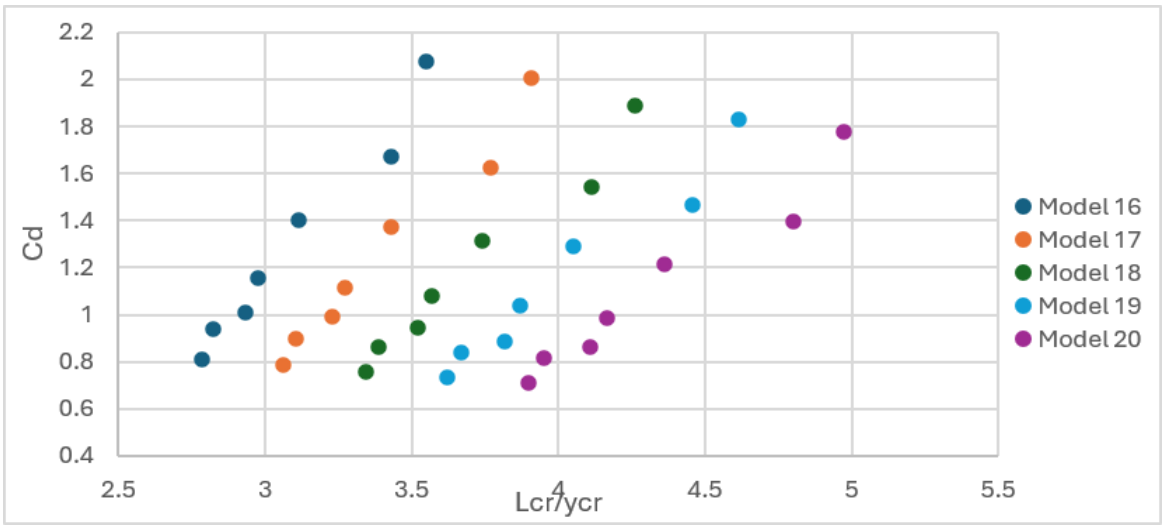

Figure 12: The relationship between C_d vs. $\frac{L_{cr}}{y_{cr}}$ for θ = 70 °

4.3 Relation of C_d vs. F_{ri}

According to flood management principles, higher Froude numbers represent more energetic conditions of flow that may reduce the efficiency of the spillway and increase hydraulic instability. This focuses the importance of controlling the conditions of approach flow to maintain optimal discharge performance during the events of extreme flood. Figures 13, 14, 15, and 16 show the negative relation between the discharge coefficient (C_d) and the Froude number due to the initial depth of the hydraulic jump generated at the stilling basin (F_{ri}) for all degrees of inclination of for the values of θ = 30°, 45°, 60°, and 70°. In general, when F_{ri} increases, C_d tends to decrease. A rapid inertia-dominated flow with an increase in the values of approach velocities is indicated when the values of F_{ri} increase. A large amount of kinetic energy is generated when the flow approaches the crest, and that leads to a change in the pressure distribution and flow patterns across the weir. As a result, the transition over the crest is smoother, the velocity distribution is more stable, and the assumptions of ideal flow conditions are more closely met. Higher values of C_d are therefore attained, and energy losses are reduced. Stronger velocity gradients and more intense turbulence result from the flow becoming more supercritical upstream as F_{ri} rises. The fast approach velocity diminishes the crest's ability to control the flow and results in an uneven flow distribution. Some of the upstream kinetic energy is lost due to internal mixing and turbulence, due to the flow being more effective over the crest. As a result, the effective head decreases, which decreases the value of C_d. In model number sixteen, the maximum value of F_{ri} was 4.38, while the value of C_d was 0.807. While model no. 5 had a minimum value of 2.83 for F_{ri} and a value of 1.465 for C_d.

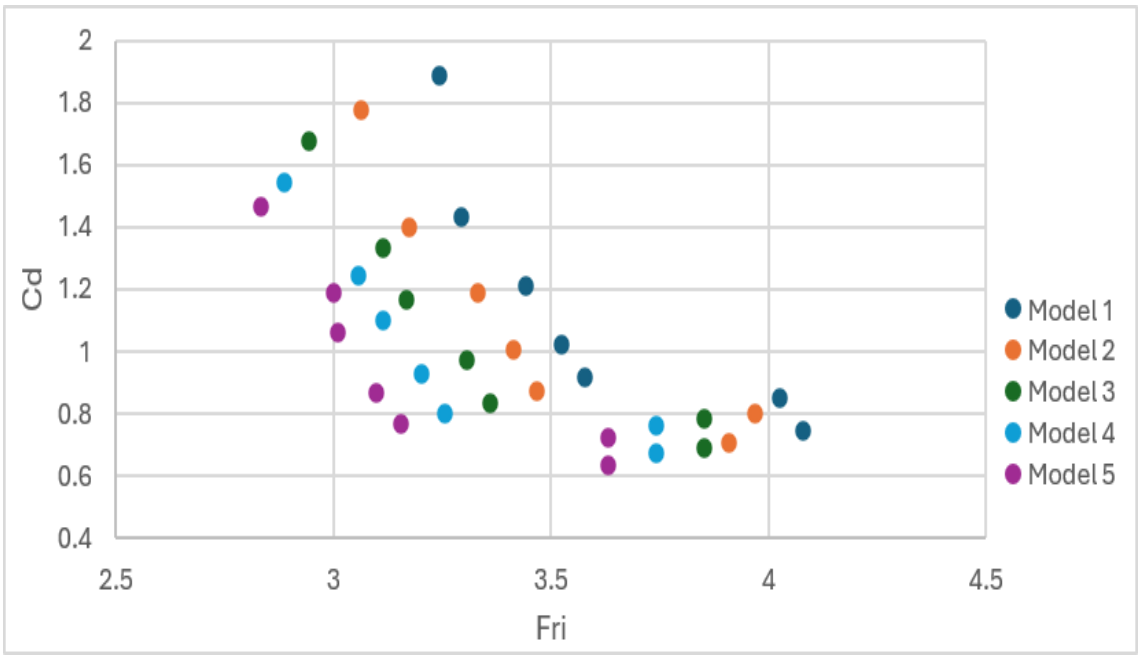

Figure 13: The relationship between C_d vs. F_{ri} for θ = 30 °

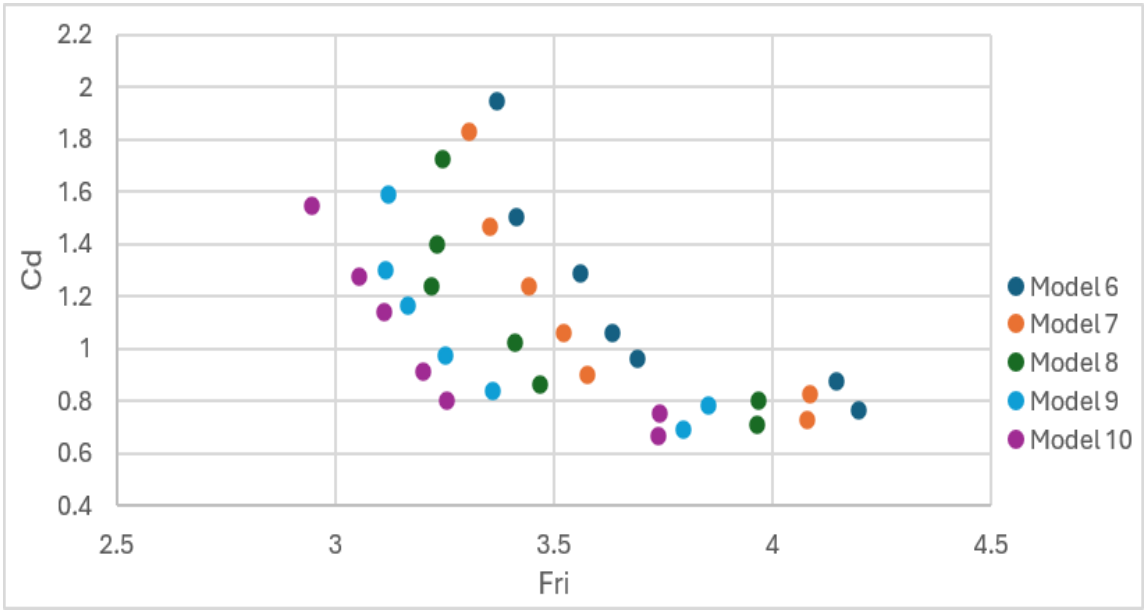

Figure 14: The relationship between C_d vs. F_{ri} for θ = 45 °

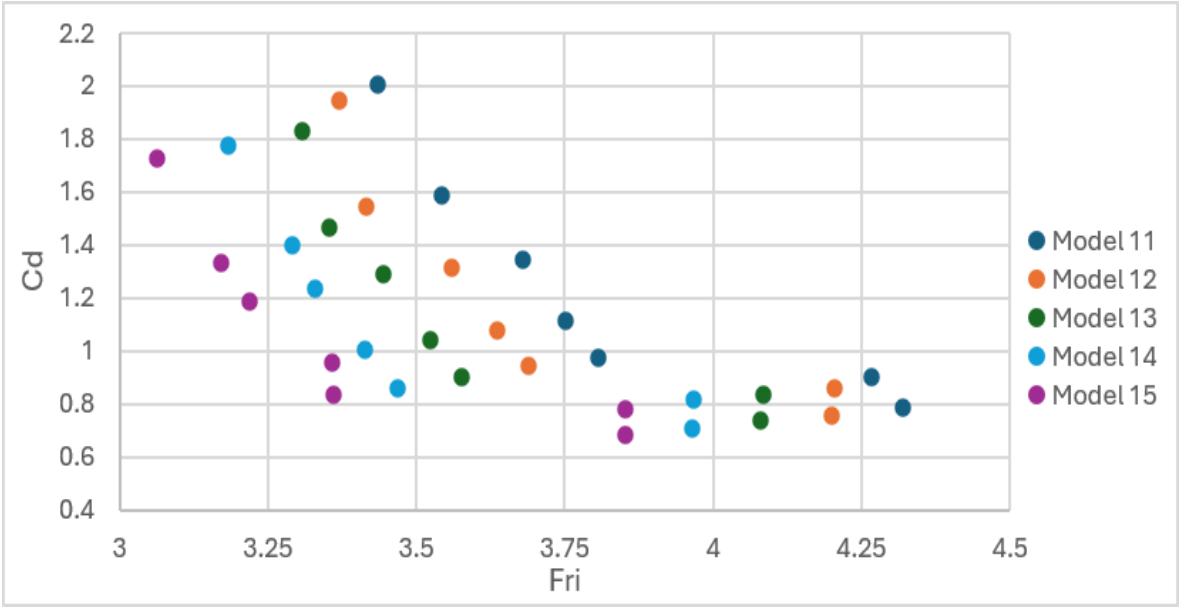

Figure 15: The relationship between C_d vs. F_{ri} for θ = 60 °

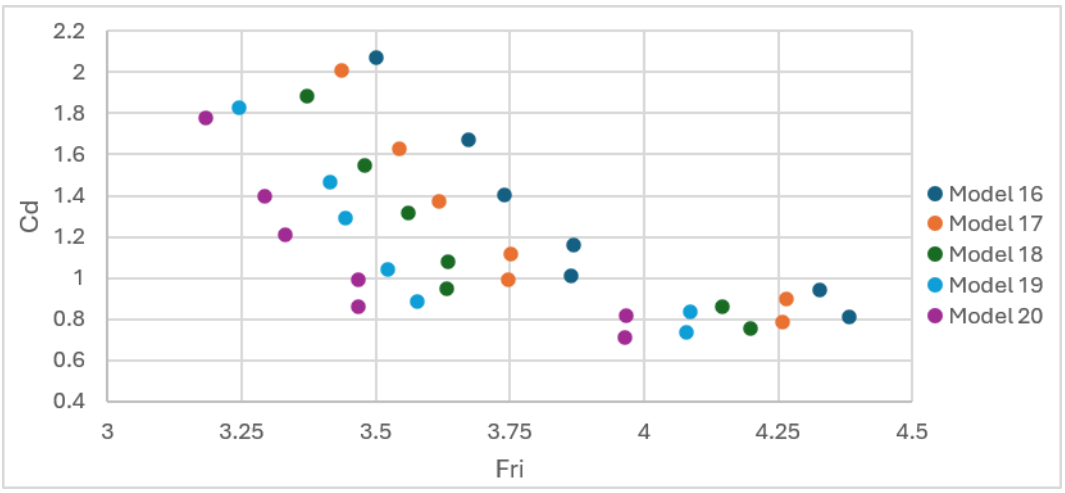

Figure 16: The relationship between C_d vs. F_{ri} for θ = 70 °

4.4 Relation of C_d vs. $\frac{L_j}{L_b}$

In hydraulic engineering applications, a longer hydraulic jump reflects higher incoming levels of energy, which may indicate inefficient control of upstream flow. This condition can adversely affect the overall spillway performance during flood discharge, emphasizing the need for integrated design between the crest of the spillway and the stilling basin.

The relationship between the discharge coefficient (C_d) and the relative jump length (L_j/L_b) is negative as shown in Figures 17, 18, 19, and 20 for the values of θ = 30°, 45°, 60°, and 70°. This suggests that when the length of the hydraulic jump increases, C_d values decrease. A longer hydraulic jump usually results in slower and more extended energy dissipation, which is frequently referred to more severe conditions of supercritical field upstream of the jump and incoming flow momentum increased.

When the value of L_j/L_b decreases, the hydraulic jump is comparatively shorter in length, suggesting that energy dissipation is more effective. Decreasing values of approach velocities and better-regulated flow conditions are typically linked by a satisfying condition, which makes the crest more efficient, and the head loss decreases. The hydraulic jump gets longer and more spread out when L_j/L_b increases, when the flow has greater kinetic energy and momentum. For such conditions, the flow is more turbulent, mixing, and energy dissipation.

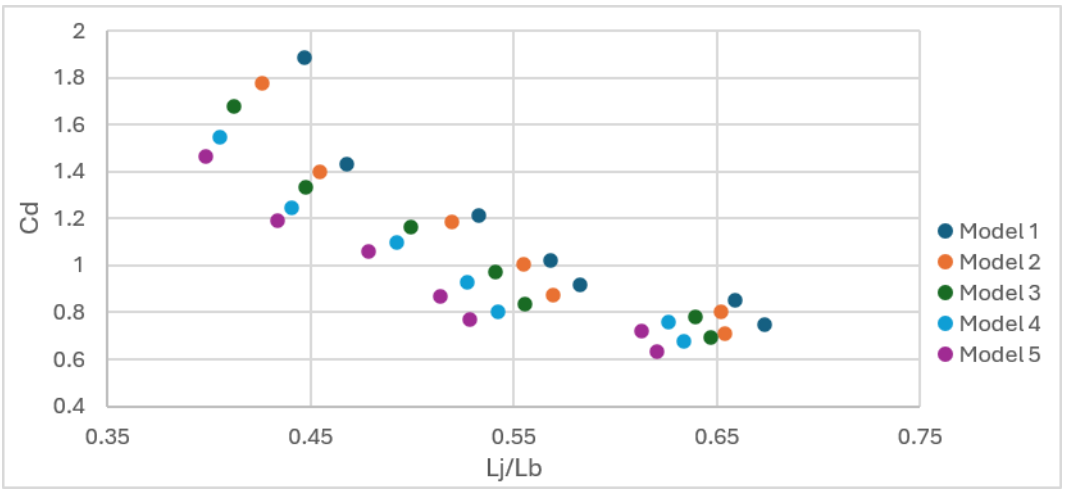

Figure 17: The relationship between C_d vs. $\frac{L_j}{L_b}$ for θ = 30 °

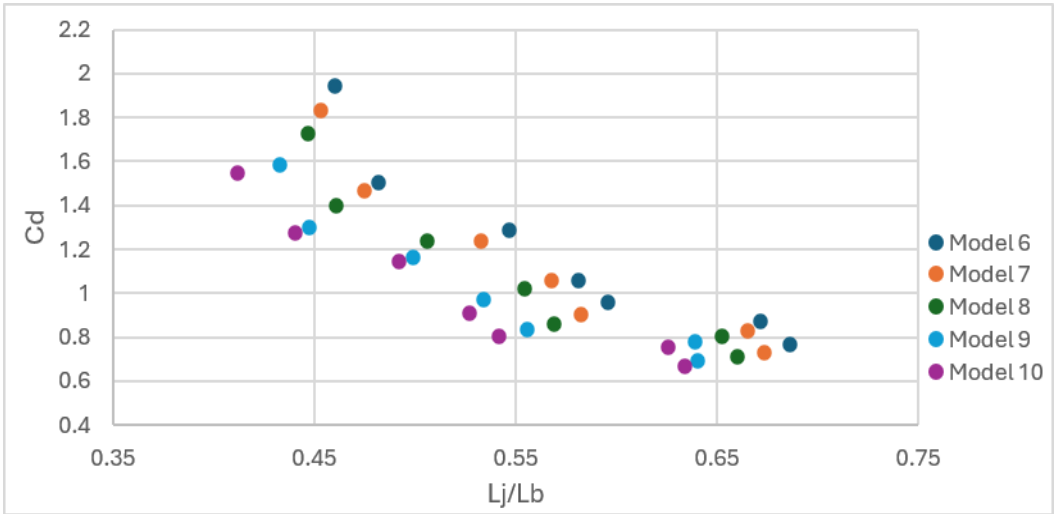

Figure 18: The relationship between C_d vs. $\frac{L_j}{L_b}$ for θ = 45 °

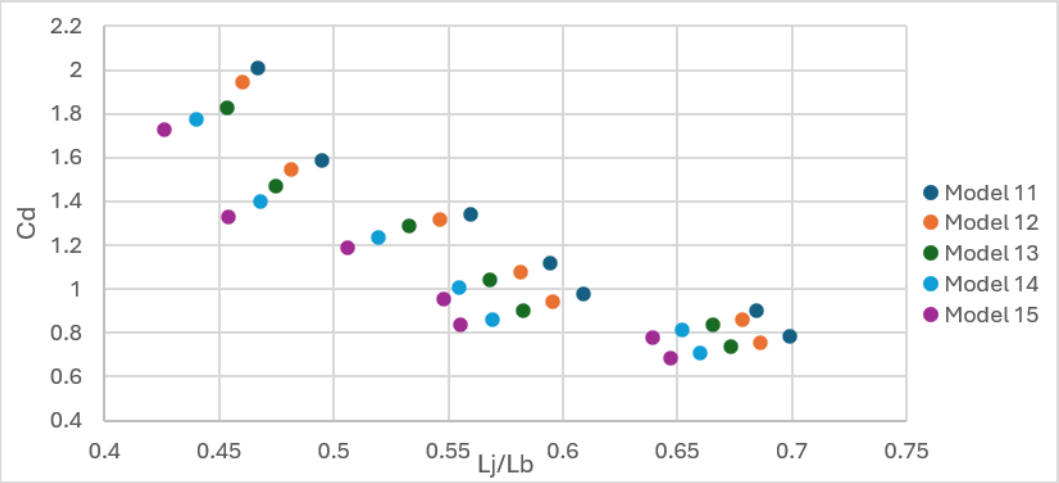

Figure 19: The relationship between C_d vs. $\frac{L_j}{L_b}$ for θ = 60 °

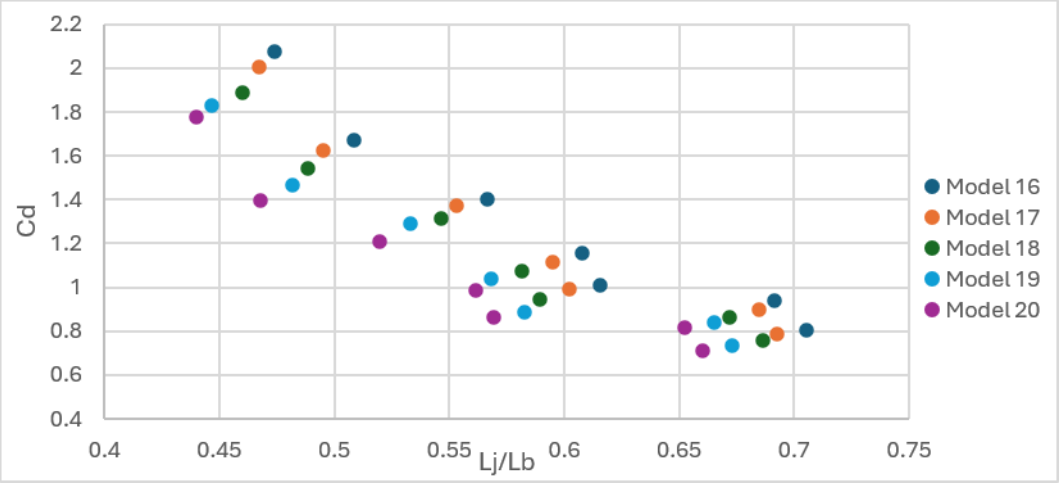

Figure 20: The relationship between C_d vs. $\frac{L_j}{L_b}$ for θ = 70 °

5. Deriving A New Formula

Equation (4) is obtained by using the experimental results for dimensional analysis parameters as input data in IBM Statistics SPSS 26 and for nonlinear regression analysis (NLR) between Cd and other non-dimensional parameters.

$$C_d = 1.747 - 2.885 * \left(\frac{H_{cr}}{P}\right) - 0.014 * \left(\frac{L_{cr}}{y_{cr}}\right) + 8.5 * 10^{-5} * \theta + 0.757 * Fr_i - 4.432 * \left(\frac{L_i}{L_b}\right) \quad (4)$$

This formula's coefficient of determination (R^2) is 0.955.

6. Comparison Between Calculated Values and Observed Values of C_D

Eighty percent of the laboratory results were used to derive a mathematical model (Eq. 4) from Table 1 in the previous sections; the remaining twenty percent were used as input data to forecast the accuracy of Eq. 4. "Calculated values of C_d" are the results of the formula.

The outcomes of the experiment were contrasted with these findings. As indicated in Table 2, the formula's correctness is indicated by the percentage difference between the two sets of data.

Table 2: A comparison between the observed and calculated values of C_d

C_d (Observed)	C_d (Calculated from eq. 4.1)	Difference Percentage %	C_d (Observed)	C_d (Calculated from eq. 4.1)	Difference Percentage %
1.0221	1.0381	1.5357	1.2362	1.2056	2.5364
1.2116	1.2523	3.253	0.972	0.9446	2.8974
1.0049	1.001	0.3952	1.1647	1.1629	0.1516
1.1877	1.213	2.0836	0.9113	0.8942	1.9018
0.972	0.9571	1.554	1.1423	1.1395	0.2522
1.1647	1.166	0.1137	1.1159	1.142	2.2876
0.9258	0.9064	2.1391	1.0767	1.0905	1.2653
1.0998	1.1239	2.1506	1.0398	1.0416	0.1722
0.8697	0.8489	2.4491	1.0049	0.9952	0.9784
1.0598	1.0834	2.1836	0.9562	0.9523	0.4124
1.058	1.0841	2.4082	1.1574	1.1927	2.9581
1.2881	1.3099	1.6643	1.1159	1.1387	2.0031

Table 2 (Cont): A comparison between the observed and calculated values of C_d					
1.058	1.0538	0.3984	1.0767	1.0872	0.9642
1.2362	1.2585	1.773	1.0398	1.0383	0.1466
1.0221	1.0074	1.461	0.9882	0.9941	0.5864

Table 2 shows that the values calculated using Eq. 4 and the observed values from the laboratory results are sufficiently consistent. Eq. 4 is highly accurate, as evidenced by the largest significant difference percentage of 3.253% between computed and observed values.

7. Conclusions

The results provide valuable guidance for hydraulic engineers in the design of chute spillways. The observed influence of the inclination of the downstream face and crest geometry on the coefficient of discharge highlights the importance of geometric configuration in achieving efficient conveyance of flow. From a flood management perspective, maximizing the coefficient of discharge allows spillways to pass higher values of discharge at lower upstream heads, thereby reducing the hazards of overtopping and improving the safety of the dam. Additionally, optimizing the length of the crest and slope can enhance the stability of the flow and minimize the energy losses, contributing to more efficient water infrastructure systems. These results can support decision-making in the design of such hydraulic structures as well as the rehabilitation of existing structures, particularly in regions subjected to extreme hydrological events. The following conclusions are observed:

- While the water surface elevation over the crest (H) is almost constant for a fixed discharge, increasing the crest length stabilizes the flow over the spillway, leading to a minor increase in the upstream depth (y_i) at the toe. As a result, the hydraulic jump shows an enhanced discharge coefficient (C_d), a slower transition to subcritical flow, and a smaller sequent depth (y_s).
- The flow channel over the spillway lengthens as the crest length does, adding more flow resistance. This raises the water surface elevation (H) and increases the upstream depth (y_i) at the toe by allowing water to build up slightly above the crest. As a result, the discharge coefficient (C_d) increases while the hydraulic leap downstream shows a somewhat smaller sequent depth (y_s) and a more gradual transition to subcritical flow.
- The combined impacts of increased flow thickness, increased turbulence, divergence from ideal pressure conditions, and the onset of submergence influence all of which work to lower the hydraulic efficiency of the weir, and are mainly responsible for the decrease in C_d with rising H_{cr}/P.
- While increasing L_{cr}/y_{cr} tends to enhance discharge efficiency and flow regulation, its impact on C_d is still minor in comparison to more important factors like H_{cr}/P. As a result, when calculating the discharge coefficient, L_{cr}/y_{cr} should be viewed as a contributing factor rather than the main regulating variable.
- Because of increased turbulence, uneven velocity distribution, and ineffective energy conversion, increasing F_{ri} causes C_d to decrease. It is a minor but crucial variable in determining the total discharge behavior, though, as its impact is still combined with other geometric and hydraulic factors.
- The inverse relation between C_d and Fri is consistent with a longer hydraulic leap, which indicates a more energetic upstream flow (higher F_{ri}). An extended jump's higher turbulence and energy losses lower the effective head that contributes to discharge over the crest, which lowers C_d.

Overall, the study demonstrates that enhancing the geometry of the spillway not only improves hydraulic performance but also contributes directly to enhancing the efficiency of flood management and the operational reliability of the systems of water infrastructure.

References

Aguilera, E. and Jimenez, O., 2019. Applicability of a 3D numerical model for flow simulation of spillways. In Proceedings of the 38th IAHR World Congress, Panama City, Panama, pp.11.

Arora, K. R., 2005. Fluid mechanics, hydraulics and hydraulic machines. Standard Publishers Distributors.

Bos, M.G., 1976. Discharge Measurement Structures. Publication No. 161, Delft Hydraulic Laboratory, Delft, The Netherlands.

Chanson, H., 2004. The hydraulics of open channel flow: An introduction (2nd ed.). Butterworth-Heinemann.

Chaokitka, S. and Chanson, H., 2022. Hydraulics of a broad-crested weir with rounded edges: physical Modelling. Hydrology and Water Resources Symposium. ISBN: 978-1-925627-64-0.

Chow, V. T., 1998. Open Channel Hydraulics, McGraw-Hill, ISBN 07-010776-9, 1988.

Eshrati, T., Fazloula, R., Sanei, M. and Emadi, A., 2015. Laboratory study of hydraulic performance of ogee spillway and downstream canal with axial arc. Journal of Water and Soil, 29(4), pp. 874–885.

Govinda Rao, N. S., and Muralidhar, D., 1963. Discharge characteristics of weirs of finite-crest width. La Houille Blanche, (5), pp. 537–545.

Henderson, F. M., 1966. Open channel flow (Vol. 522). New York: Macmillan.

Kumcu, S. Y., 2017. Investigation of Flow Over Spillway Modeling and Comparison between Experimental Data and CFD Analysis. KSCE Journal of Civil Engineering,21(3), pp. 994-1003.

Rajaratnam, N., 1990. Skimming flow in stepped spillways. Journal of Hydraulic Engineering, 116(4), 587–591.

RECLAMATION, U. B. O., 2001. Water measurement manual. US Government Printing.

Rendón, V., Sánchez-Juny, M., Estrella, S., Sanz-Ramos, M., Rucano, P., and Huarca Pulcha, A., 2023. Discharge coefficients of standard spillways at high altitudes. Preprints. https://doi.org/10.20944/preprints202312.1084.v1.

Salmasi, F., and Abraham, J., 2022. Discharge coefficients for ogee spillways. Water Supply,22(5).

Sheikh Kazemi, J. and Saneie, M., 2014. The effect of approach channels on the discharge of ogee spillway in the axial arc condition with convergent sidewalls. Journal of Middle East Applied Science and Technology, 22(2), pp.119-123.

Varcin, H. et al., 2025. Examination of Flow in a Chute Spillway During Flood Conditions Using a 3D Numerical Model. Journal of Flood Risk Management, 18(4).